Biosensors and Bioelectronics 54 (2014) 222–228

Contents lists available at ScienceDirect

Biosensors and Bioelectronics

journal homepage: www.elsevier.com/locate/bios

Hydrogel with chains functionalized with carboxyl groups as universal 3D platform in DNA biosensors

Agata Kowalczyk, Michal Fau, Marcin Karbarz, Mikolaj Donten, Zbigniew Stojek, Anna M. Nowicka *

Faculty of Chemistry, University of Warsaw, Ul. Pasteura 1, 02-093 Warsaw, Poland

ARTICLE INFO

Article history:
Received 23 July 2013
Received in revised form
4 November 2013
Accepted 5 November 2013
Available online 14 November 2013

Keywords:
Hydrogel
DNA biosensor
Electrochemical quartz crystal microbalance
Electrochemical impedance spectroscopy
Scanning electron microscopy

ABSTRACT

Application of hydrogel based on *N*-isopropylacrylamide with carboxyl groups grafted to the chains enabled the immobilization of DNA at an extent exceeding that for flat surfaces by at least one order of magnitude. The probe DNA strands in the 3D platform were fully available for the hybridization process. The examination of the gels containing different amounts of grafted carboxyl groups (1–10%) was done using quartz crystal microbalance, electrochemical impedance spectroscopy, chronoamperometry and ionic coupled plasma with laser ablation. The optimal carboxyl group content was determined to be 5%. A very good agreement of the data obtained with independent techniques on content of DNA in the gel was obtained. In comparison to the other methods of immobilization of DNA the new platform enabled complete removal of DNA after the measurements and analysis and, therefore, could be used many times. After a 10-fold exchange of the DNA-sensing layer the efficiency of hybridization and analytical signal did not change by more than 5%. The sensor response increased linearly with logarithm of concentration of target DNA in the range 1×10^{-13}–1×10^{-6} M. The obtained detection limit was circa 8×10^{-13} M of target DNA in the sample which is a substantial improvement over the planar sensing layers.

1. Introduction

Selective immobilization of nucleic acids is a very essential step for many applications including clinical diagnostic (Huang et al., 2011), biosensor development (Baeissa et al., 2012; Zhou et al., 2013), biomaterials design (Park et al., 2007) and nanotechnology (Taton et al., 2000). The traditional methods of attachment of nucleic acids include physical adsorption (Wang et al., 1998; Wang et al., 2000), covalent binding (Gallardo et al., 2006; Adenier et al., 2004) and encapsulation (Lomas et al., 2007; Zelikin et al., 2007). The physical adsorption does not require the pre-functionalization of the substrate on which the immobilization of DNA takes place. Contrary, the covalent linkage involves the functionalization of the substrate and DNA. Several functional groups, including carboxylic acids, quinones, hydroquinones, phenols, peroxides, aldehydes, ethers, esters, ketones, and alcohols, which could interact and stabilize the adsorbed DNA molecules and improve the ET rate can be used (Pividori and Alegret, 2005). A serious limitation of the conventional methods of DNA immobilization is the lack of universality regarding the substrate material. A smart, hydrogel platform for biochemical applications was already used as a platform for biomolecules (Tan et al., 2012; Adhikari and Banerjee, 2010; He et al., 2010; Kopeček, 2007; Wang et al., 2011; Adhikari and Banerjee, 2011).

In this paper we demonstrate that the application of the hydrogels with the polymer chains grafted with carboxyl groups leads to effective DNA immobilization via highly specific interactions. It is known that the quality of a DNA biosensor is determined by, among others, its detection limit, what is in a direct correlation with the number of probe DNA strands present in the sensing layer and able to hybridize with the examined DNA. The traditional ways of DNA immobilization in the sensing layer (via either thiol or phenyl linkers) permit to obtain circa 1×10^{12} of DNA strands at the transducer platform with the hybridization efficiency of circa 80% (Kowalczyk et al., 2012). In such platforms it is important that the distribution of DNA strands in the sensing layer is uniform. The polymeric hydrogels, i.e., cross-linked hydrophilic polymer networks filled with an aqueous solution, could eliminate this restriction due to their unique structure. In the swollen state they are soft and rubbery and are well penetrable by small molecules. They resemble living tissues and some of them possess excellent biocompatibility (Yang, 2008). In this study only oligonucleotides of equal length were examined. A difference in length leads to the formation of overhangs (Shamsi and Kraatz, 2011).

2. Experimental

2.1. Materials and methods

All chemicals were of the highest purity available. KOH (p.a., POCH, Poland), KH_2PO_4 (p.a., POCH, Poland), HCl (p.a., POCH,

* Corresponding author.
E-mail address: anowicka@chem.uw.edu.pl (A.M. Nowicka).

0956-5663/$ - see front matter © 2013 Elsevier B.V. All rights reserved.
http://dx.doi.org/10.1016/j.bios.2013.11.017

Poland), $K_3[Fe(CN)_6]$ (p.a., POCH, Poland), $K_4[Fe(CN)_6]$ (p.a., POCH, Poland), *N*-hydroxysuccinimide (NHS; Sigma), *N*-(3-dimethylaminopropyl)-*N*′-ethylcarbodiimide hydrochloride (EDC; Sigma), *N*-isopropylacrylamide (NIPA; Aldrich), acrylic acid (AA; Sigma), *N*,*N*′-methylenebisacrylamide (BIS; Aldrich), ammonium persulfate (APS; Aldrich) and *N*,*N*,*N*′,*N*′-tetramethylethylenediamine (TEMED; Aldrich) were used as received. Immobilization buffer: 0.02 M HEPES (2-[4-(2-hydroxyethyl)piperazin-1-yl]ethanesulfonic acid), pH 7.4. Hybridization buffer: 0.02 M HEPES buffer, pH = 7.4 with 1 M NaCl and 1 mM EDTA.

The primary oligonucleotide sequence was taken from a strain of lactic acid bacteria of the genus *Lactococcus lactis*. Their natural environment is the human digestive system (esophagus). They can be found in various foods such as leaven, cheese and yogurt. The following oligonucleotide sequences were used:

- probe DNA: (5′–3′): H_2N-C6-CGCCAACGTTTTCGC CAACG
- complementary target DNA (5′–3′): CGTTGGCGAAAA-CGTTGGCG (designed from the gene of *Lactococcus*, a common milk bacteria)
- non-complementary DNA strand (5′–3′): CGCCAACGTTTT-CGCCAACG.

2.2. Gels synthesis

Gels were synthesized by free-radical solution copolymerization of *N*-isopropylacrylamide, acrylic acid and *N*,*N*′-methylenebisacrylamide. The total concentration of NIPA, AA and BIS was constant as 700 mM. BIS concentration in all samples was kept at 7 mM, while the concentrations of NIPA and AA were varied. The pre-gel solutions were degassed and the polymerization was initiated and accelerated by ammonium persulfate (1.88 mM) and *N*,*N*,*N*′,*N*′-tetramethylethylenediamine (32 mM), and was carried out at 20 °C for 20 h.

The percentage of acrylic acid in the gel, $Y_{solution}$, using the pre-gel solution composition is defined as follows:

$$Y_{solution} = \frac{n_{AA}}{n_{NIPA} + n_{AA} + n_{BIS}} 100\% \quad (1)$$

In this paper $Y_{solution}$ equaled 10, 5, 2.5, 1 and 0%.

2.3. Electrochemical measurements

Cyclic voltammetry (CV), chronoamperometry (CA) and electrochemical impedance spectroscopy (EIS) were performed using an Autolab, model PGSTAT 30 potentiostat equipped with an ECD amplifier module (noise-filter RC time settings: 0 s for scan rates > 10 mV/s and 0.1 s for scan rates < 10 mV/s) and the electrochemical analysis system based on the GPES or FRA software package (Eco Chemie B.V., Utrecht, Netherlands). The impedance spectra were obtained for the frequency range from 0.05 Hz to 100 kHz with the ac amplitude equal to 5 mV. The fitting of the experimental data to the appropriate equivalent circuit was performed using the Complex Nonlinear Least–Squares (CNLS) method. For electrochemical measurements the three-electrode system consisting of a gold disc electrode (1.6 mm in diameter, BAS, UK) used as the working electrode, a Ag/AgCl/3 M KCl reference electrode and a platinum wire used as the auxiliary electrode were employed. The surface of the working electrode was polished with 1- and 0.3-μm Al_2O_3 powder on a wet pad. After each polishing, to remove alumina completely from the electrode surface, the electrode was rinsed with a direct stream of ultrapure water (Milli-Q, Millipore, conductivity of ~0.056 μS/cm) and dried. Next, the electrode was cycled between −0.3 V and 1.5 V (vs. Ag/AgCl) in 0.1 M H_2SO_4 solution until a stable voltammmogram typical for a clean gold electrode was obtained (Finklea et al., 1987). During all experiments, the electrochemical cell was kept in a Faraday cage to minimize the electrical noise.

For EIS measurements the gel pieces were first soaked in 0.02 M PBS buffer containing equimolar concentrations (5 mM) of $Fe(CN)_6^{3-/4-}$. Next a piece of gel was placed in a home-made special electrochemical cell between two planar electrodes: working and auxiliary/reference. For the experiments with DNA sequences the samples were soaked in the solution containing the appropriate sequences at concentration 10 μM.

2.4. EQCM measurements

An electrochemical quartz crystal microbalance, model Autolab with 6-MHz Au/TiO_2 quartz crystal resonators, was used in this study. The EQCM technique allowed us to record simultaneously voltammetric/chronoamperometric and microgravimetric curves. The resonant frequency of the quartz crystal lattice vibrations in a thin quartz crystal wafer was measured in function of the mass attached to the crystal interface. For a thin rigid films, the interfacial mass change, Δm, is related to the shift in resonance oscillation frequency, Δf, of the EQCM through the Sauerbrey equation (Hepel, 1999; Bruckenstein and Shay, 1985; Sauerbrey, 1959):

$$\Delta f = -\frac{2\Delta m n f_0^2}{A\sqrt{\mu_q \rho_q}} \quad (2)$$

where f_0 is the oscillation frequency in the fundamental mode, n is the overtone number, A is the piezoelectically active surface area, ρ_q is the density of quartz ($\rho_q = 2.648\ g\ cm^{-3}$), and μ_q is the shear modulus of quartz ($\mu_q = 2.947 \times 10^{11}\ g\ cm^{-1}\ s^{-2}$). All experimental variables influencing the resonant frequency of the EQCM electrodes such as the temperature, pressure, viscosity and density of the solution, were kept constant during the measurements. The piezoelectrically active (geometrical) surface area of the working Au electrode was 0.3523 cm^2 and the real surface area $A = 0.5286\ cm^2$ (roughness factor $R = 1.5$). The real surface area of the Au-EQCM electrode was determined from the Pb upd voltammetric peaks. The deposition solution was 0.01 M lead(II) perchlorate in 0.1 M perchloric acid. The theoretical value for the Pb monolayer on Au is $Q_{Pb} = 302\ \mu C\ cm^{-2}$. The piece of the gel has the shape of a cylinder, which is tightly fitted to the gold quartz crystal.

2.5. SEM and ICP MS with laser ablation measurements

The morphologies of the pure gel and the gel with DNA were characterized using scanning electron microscopy (FESEM) (Merlin; Carl Zeiss Germany; with primary electron beam energy 5 keV). The amount of ^{31}P in the gel before and after hybridization process were obtained from the laser ablation ICP MS measurements; three laser linear scans were applied.

2.6. Preparation of biosensor

Each final analytical measurement was preceded by immobilization and detection of DNA step sat the same sample of gel (NIPA with 5% –COOH groups). The QCM results clearly showed that the NIPA gel containing carboxyl groups was capable of specific DNA immobilization. All experiments were performed at room temperature (21 ± 1 °C). The preparation of the electrochemical DNA hybridization sensor involved several steps listed below. Typical EQCM response curves obtained after each step of NIPA-gel modification are presented in Fig. 1. The data presented in Fig. 1 were corrected by subtracting the signal corresponding to 5% NIPA gel swelled with pure HEPES buffer.

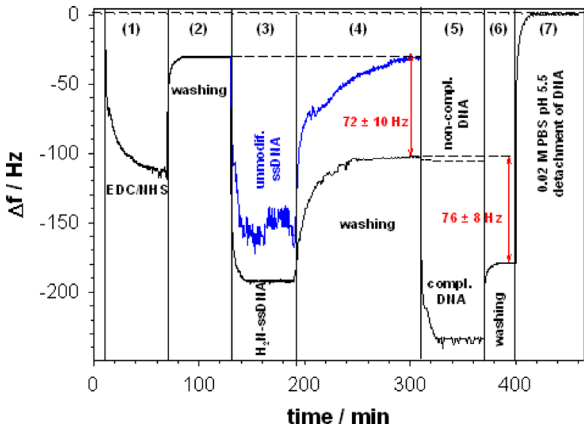

Fig. 1. Typical responses of QCM during each step of modification of NIPA containing 5% of –COOH groups: (1) activation of carboxyl groups; (2) washing; (3) immobilization of unmodified (blue line) and amino-modified ssDNA (black line); (4) washing; (5) hybridization with non-complementary (dashed line) and complementary DNA (solid line); (6) washing; (7) hydrolysis of peptide bond – detachment of DNA. The steps are separated with vertical lines. (For interpretation of the references to color in this figure caption, the reader is referred to the web version of this article.)

2.6.1. Activation of the carboxyl groups

The attachment of H_2N-ssDNA to carboxyl groups in NIPA gel was treated according to the procedure described in the literature (Liu et al., 2005). The modified piece of gel was kept in an aqueous solution of 10 mM NHS and 40 mM EDC for 1 h. Then the piece of the gel was washed in the pure HEPES buffer to remove unreacted reagents from the gel channels.

2.6.2. H_2N-ssDNA probe immobilization

After 1 h activation the hydrogel was treated with a solution containing an excess of H_2N-ssDNA strands (10 μM in 0.02 M HEPES buffer, pH=7.4) vs. the content of the carboxyl groups. To prove the existence of specific interactions between the carboxyl groups of the gel and the amine groups of DNA the unmodified ssDNA was examined. In such a case no change in the resonant frequency was observed, see Fig. 1. To be sure that the DNA strands present in the gel matrix are bound only through the peptide bond the polymer with immobilized biomolecules was immersed into pure HEPES buffer. For 2 h, every 10 min, 1 ml of HEPES buffer was removed and fresh buffer of the same volume was added. During this operation a continuous increase in frequency was observed. The washing step was finished after reaching the stabilization of the frequency. A stable value of frequency meant that unbound DNA strands were completely removed from the polymer matrix. At this point the sensor was ready for the hybridization process.

2.6.3. Hybridization

Each hydrogel sample with immobilized ssDNA was immersed in the hybridization buffer solution containing the target DNA at the appropriate concentration for 60 min. After completing this step the hydrogel piece was washed with pure HEPES buffer to remove non-hybridized DNA strands from the hydrogel matrix.

2.6.4. Determination of the amount of the DNA molecules bound to the carboxylic groups in the gel

The amount of DNA molecules immobilized in the polymer matrix was determined from the number of $Ru(NH_3)_6^{3+}$ molecules electrostatically bound with DNA according to the procedure described in the literature (Steel et al., 1998). In those experiments with the hydrogels containing single- and double-stranded DNA the chronocoulograms were obtained in 0.02 M HEPES buffer containing 0.15 M NaCl and 2 mM KCl and in the same buffer with 50 μM $Ru(NH_3)_6^{3+}$. Finally, the calculation of the number of DNA molecules effectively immobilized in NIPA gel was done using the equation:

$$\gamma_{DNA} = \gamma_{Ru(NH_3)_6^{3+}} \left(\frac{z\, N_A}{m} \right) \tag{3}$$

where $\gamma_{Ru(NH_3)_6^{3+}}$ is the number of $Ru(NH_3)_6^{3+}$, z is the charge of the redox molecule ($z=3$), N_A is Avogadro's number, and m is the number of the bases in probe DNA ($m=20$).

2.6.5. Immobilization of gel film on QCM electrode

The gels were synthesized in a teflon tube of inner diameter identical to the QCM electrode size. After synthesis the gel samples were carefully cut into equal, thin and smooth slices. The mass of the soaked slice should not be bigger than 20 mg. Otherwise the usefulness of QCM would be limited. Controlled experiments were done to prove that the gel films were ideally adhered to the gold surface.

3. Results and discussion

3.1. EIS characteristics of gel platform

The first task was to examine the ability of the amine-modified DNA sequence to bind specifically to the hydrogels through carboxyl groups. NIPA hydrogels with various percentage of the carboxyl groups were used (1–10%).

Application of the hydrogel platform in the electrochemical DNA detection required electrochemical characterization of the hydrogel. For this purpose the electrochemical impedance spectroscopy technique (EIS) was applied. This technique is a sensitive method, and enables a deep insight in the interfacial structure. In the EIS studies we used a standard redox probe: a mixture of ferricyanide and ferrocyanide anions (equimolar ratio). Fig. 2 presents exemplary impedance plots obtained in 5 mM $Fe(CN)_6^{3-/4-}$ at the formal potential of the couple for the hydrogel with selected percentage of carboxyl groups. For quantitative description of the EIS results we used a simple Ershler–Randles equivalent circuit (inset in Fig. 2) (Kowalczyk et al., 2011; Lasia, 2009; Brug et al., 1984).

Since the presented Nyquist plots are characterized by a semicircle followed by a straight line at 45 deg which is typical for diffusion controlled processes, therefore, to obtain the detailed information from the impedance spectroscopy data a simple Ershler–Randles equivalent circuit was selected for the fitting to the experimental results.

In the presence of semi-infinitive diffusion the mass transfer Warburg impedance Z_W is described by the following:

$$Z_W = \sigma \omega^{-1/2} (1-j) \tag{4}$$

where the Warburg parameter, σ, is given by the following:

$$\sigma = \frac{RT}{\sqrt{2} n^2 F^2} \left[\frac{1}{\sqrt{D_O C_O^*}} + \frac{1}{\sqrt{D_R C_R^*}} \right] \tag{5}$$

D_i and C_i^* are diffusion coefficients and bulk concentrations of both oxidized (O) and reduced (R) forms of the redox species. Other symbols have their usual meaning.

The Ershler–Randles circuit led to a good fit when the double-layer capacitance was replaced by a constant phase element (CPE), which is the appropriate action for solid electrodes. The

impedance of this element is described by the following:

$$Z_{CPE} = T^{-1}(j\omega)^{-\phi} \quad (6)$$

where ω is the angular frequency, $j=(-1)^{1/2}$ and ϕ is the exponential factor of the phase element CPE. The average double layer capacitance can be then estimated from (Brug et al., 1984):

$$T = C_{dl}^{\phi}(R_s^{-1}+R_{ct}^{-1})^{1-\phi} \quad (7)$$

where R_s and R_{ct} are the solution resistance and the resistance of the charge transfer, respectively. From the EIS experiment the electron-transfer rate constant, k_0, was also determined (the data are presented in Table 1) using the formula:

$$k_0 = \left(\frac{\sigma}{R_{ct}}\right)/\frac{2\xi^{\alpha}}{\sqrt{2D_{ox}}} \quad (8)$$

where k_0 is electron-transfer rate constant, $\xi = \sqrt{D_{ox}/D_{red}} \approx 1$ for $Fe(CN)_6^{3-/4-}$ species, α is transfer coefficient and is assumed to equal 0.5, D_{ox} is diffusion coefficient of $Fe(CN)_6^{3-}$ (D_{ox} is taken as 0.896×10^{-5} cm^2 s^{-1} (Lide and Frederikse, 1997); since in the gel environment the value of the diffusion coefficient usually drops by less than 19% compared to the aqueous solution (Karbarz et al., 2005), therefore, the value of D_{ox} taken for calculations was 0.726×10^{-5} cm^2 s^{-1}) and R_{ct} is charge transfer resistance. k_0 can be determined directly from R_{ct} (Bard et al., 2008); however, by dividing σ per R_{ct} the electrode surface area can be eliminated.

Table 1 presents the values of the system parameters determined by fitting the circuit parameters to the experimental data.

It is clear that the electrostatic repulsions between the redox probe and negatively charged carboxyl groups increase considerably with increasing the percentage of carboxyl groups in the matrix. This effect is well visible in the changes in the value of the charge transfer resistance (Table 1). The transport of the electroactive species in the hydrogel matrix is really not affected by the increase in the amount of –COOH groups, as the Warburg parameter is nearly constant. The constant phase element represents here a "leaking" and thus not ideal capacitor, which has a non–zero real component corresponding to energy dissipation (Lasia, 2009). Just for monocrystalline (or liquid) electrodes in the absence of specific adsorption, $\phi=1$ and the purely capacitive behavior is observed. The exponent parameter ϕ is usually smaller than 1. The solution resistance, R_s, for all measurements, was equal circa 6 Ω cm^2. From Table 1 it follows that the exponential factor (ϕ) of constant phase element, after modification of the electrode surface by NIPA gel, slightly decreased for the gel containing 1% of the –COOH groups, and then markedly increased to the value 0.861 for other NIPA gels. The latter effect is caused by the formation of a tighter structure of the polymer. Low values of the exponential factor, ϕ, implies rather elevated values of the capacitive parameter T of the order of 70 μF s$^{(1-\phi)}$, which leads to the changes of the electrode capacitance. The increase in the double layer capacity (C_{dl}) with increasing amount of the carboxyl groups suggests accumulation of charge in the layer. The corresponding data are presented in Table 1. Contrary to the dependencies found for R_{ct} and C_{dl} the electron-transfer rate constant decreased by circa 30% when the percentage of carboxyl groups in NIPA was raised to 10.

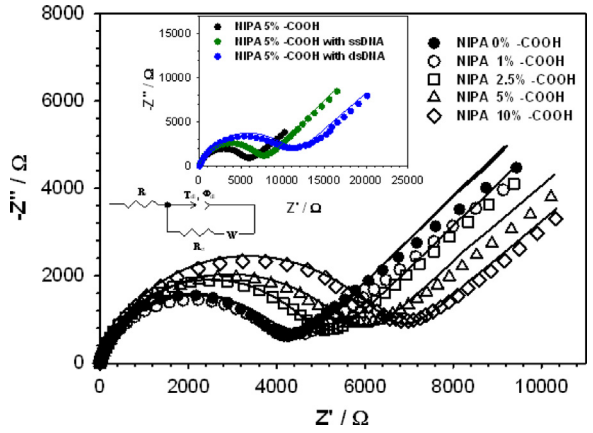

Fig. 2. Nyquist plots of pure NIPA gel (volume 0.128 cm^3) containing different percentage of –COOH groups. Experimental conditions: 0.02 M PBS buffer (pH 7.4) containing 5 mM $Fe(CN)_6^{3-/4-}$, E_{app}=245 mV, Au electrode (ϕ=1.6 mm). Upper inset: Nyquist plots of NIPA gel containing 5% of –COOH groups before and after hybridization process. Solid lines are fitted to experimental data (points). Lower inset: scheme of Ershler–Randles equivalent circuit: R_s – solution resistance; R_{ct} – charge transfer resistance; T_{dl} and ϕ_{dl} – constant phase element parameters; W – Warburg impedance.

3.2. Optimization of percentage of –COOH groups in NIPA hydrogel for effective DNA immobilization

Next we checked whether the single stranded DNA modified with the amino group (H_2N-ssDNA) and attached to the –COOH group by the peptide bond is still capable of hybridizing. The efficiency of the hybridization process was monitored by determination of the amount of the DNA molecules bound to the carboxyl groups in the specific volume of the gel. The obtained data are presented in Table 1. If H_2N-ssDNA attached to the carboxyl groups in the NIPA gel is evenly distributed and, therefore, fully accessible for the hybridization process then the number of DNA molecules after the reaction with fully complementary DNA sequence (expressed in moles of $Ru(NH_3)_6^{3+}$) should be two times higher

Table 1
Changes in impedance parameters (capacitive parameter (T) and exponential factor (ϕ) of constant phase element (CPE); resistance of the charge transfer (R_{ct}), Warburg parameter (σ) and double layer capacity (C_{dl})), electron-transfer rate constant calculated from EIS data and number of DNA molecules immobilized in NIPA gel selected volume vs. percentage of carboxyl groups.

	NIPA	NIPA 1% –COOH	NIPA 2.5% –COOH	NIPA 5% –COOH	NIPA 10% –COOH
EIS parameters					
T (μF s$^{(1-\phi)}$ cm^{-2})	30.1 ± 2.3	59.2 ± 4.1	42.7 ± 5.1	59.2 ± 4.8	58.4 ± 6.2
ϕ	0.867 ± 0.02	0.826 ± 0.03	0.861 ± 0.02	0.868 ± 0.01	0.855 ± 0.04
R_{ct} (Ω cm^2)	82.4 ± 7.2	83.8 ± 6.9	97.0 ± 8.7	114.4 ± 9.4	130.8 ± 10
σ (Ω rad$^{1/2}$ s$^{-1/2}$ cm^2)	70.9 ± 5.3	71.4 ± 4.5	69.9 ± 7.2	70.42 ± 5.3	74.9 ± 6.8
C_{dl} (μF cm^{-2})	7.32 ± 0.6	9.37 ± 1.0	9.91 ± 0.85	15.4 ± 0.7	18.8 ± 1.2
k_0 (cm^2/s)	(2.0 ± 0.2) × 10^{-3}	(2.0 ± 0.2) × 10^{-3}	(1.7 ± 0.1) × 10^{-3}	(1.4 ± 0.1) × 10^{-3}	(1.3 ± 0.3) × 10^{-3}
Chronoamperometry					
ssDNA (molecules cm^{-3})	(5.15 ± 0.2) × 10^4	(1.08 ± 0.1) × 10^{14}	(1.75 ± 0.1) × 10^{14}	(2.20 ± 0.1) × 10^{14}	(2.74 ± 0.1) × 10^{14}
dsDNA (molecules cm^{-3})	(4.82 ± 0.3) × 10^4	(1.44 ± 0.2) × 10^{14}	(3.50 ± 0.2) × 10^{14}	(4.45 ± 0.1) × 10^{14}	(4.60 ± 0.1) × 10^{14}

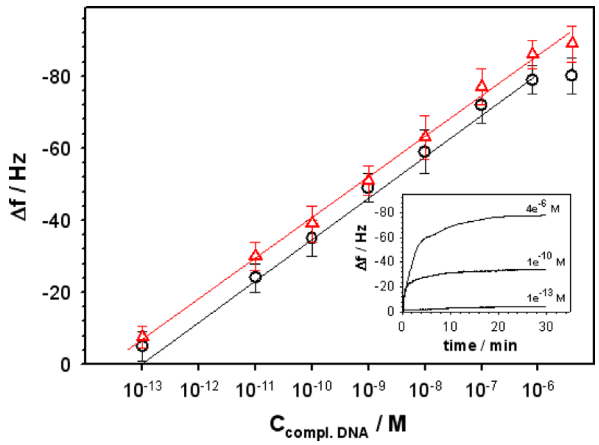

Fig. 3. Calibration plots for DNA biosensor with EQCM detection. Measurements were done with one gel sample (red triangles) and with fresh gel sample for each concentration (black cycles). Inset: example background corrected (see section 6 of Fig. 1) QCM responses for a DNA sensor after hybridization process with complementary DNA. (For interpretation of the references to color in this figure caption, the reader is referred to the web version of this article.)

than that of the ssDNA molecules. Such ideal situation took place for the NIPA gel containing 2.5–5% of –COOH groups. For the content of carboxyl groups higher and lower than the limits of this range the hybridization efficiency was substantially lower.

3.3. DNA hybridization and QCM detection

The optimal hydrogel (containing 5% of the carboxyl groups) was used in further experiments. Fig. 3 inset shows example frequency changes of the sensor after hybridization of probe DNA immobilized in the gel with completely complementary target DNA. The measurements were done either with one piece of gel or a series of fresh identical gel samples. These results were compared and no significant differences in the detection limit and the range of linearity of the calibration plot were found. The obtained calibration plots presented in Fig. 3 were constructed vs. logarithm of complementary DNA concentration in solution. The linear working concentration range extended from 1×10^{-13} to 1×10^{-6} M. The linear dependence of the sensor signal is on logarithm of concentration of complementary DNA. Such type of the dependence (analytical signal vs. log $C_{compl.\ DNA}$) is frequently seen for DNA sensors (see e.g. Patolsky et al., 2000; Steichen et al., 2007; Zhang et al., 2008). The obtained detection limit is circa 8×10^{-13} M of the complementary ssDNA strands in the sample. This value was estimated from the equation $\Delta f_{non\text{-}compl.\ DNA}+3\sigma_{\Delta f\ non\text{-}compl.\ DNA}$, where $\sigma_{\Delta f\ non\text{-}compl.\ DNA}$ is the standard deviation of the frequency shift measured upon the addition of non-complementary DNA strands.

The stability of the biosensor was examined by measuring the changes in the frequency shift in HEPES buffer every 6 h during the lab hours for 14 days. The response of the sensor was practically unchanged (standard deviation was circa 3.9%) during the first 7 days, and changed to the level of ~84% of the initial response after 7 days.

For all applied concentrations (1×10^{-13} to 4×10^{-6} M) the repeatability was good; the relative standard deviation was circa 7% ($n=5$).

Since the QCM measurements indicated that the equilibrium in the system is reached sufficiently quickly we have estimated the equilibrium constant for the hybridization reaction. For this purpose the theoretical approach of Ogi et al. (2008) was used. The measured and estimated values of equilibrium constant were 5.45×10^{7} and 5.15×10^{7} M^{-1}. The agreement is apparently satisfactory, so the hindrance effects were negligible.

Since it was possible to remove the entire sensing layer (immobilized DNA) from the gel matrix, we have done this several times. The hybridization efficiency and analytical signal did not change more than 5% after 10 removals.

3.4. Analytical performance

Due to the fact that the hydrogel containing 5% of the carboxyl groups had the best electrochemical characterization it was used in further experiments. The QCM measurements were done to proof and to demonstrate the effectiveness of immobilization of DNA in the gel matrix and in consequence the successful detection of the specific DNA sequences at low level. After addition of the complementary DNA sequence the resonant frequency decreased. From the QCM data we have calculated the maximal amount of DNA bound in the polymer matrix. In the experiments a synthetic DNA sequence was used, so the DNA molecular mass was known. The number of DNA molecules specifically immobilized in the polymer matrix per volume of the piece of gel was:

$$\gamma_{H_2N-ssDNA}=\frac{4.3\times10^{-9}\cdot(-\Delta f)\cdot N_A}{M_{H_2N-ssDNA}\cdot V_{gel}} \quad (9)$$

where N_A is the Avogadro Number, $M_{H_2N-ssDNA}$ is the molecular mass of the oligonucleotide and V_{gel} is the volume of the gel sample (0.128 cm^3). The apparent mass increase related to the observed experimental frequency shift for H_2N-ssDNA attached to the carboxyl group in polymer matrix was $(2.31\pm0.3)\times10^{14}$ molecules cm^{-3}. During the hybridization process $(2.47\pm0.2)\times10^{14}$ molecules cm^{-3} of the complementary ssDNA was bound. It meant that virtually all ssDNA strands immobilized in the polymeric matrix took part in the hybridization process. Since the attachment of DNA strands it done through the peptide bond it is to hydrolyze that bond in an weakly acidic medium and, therefore, to exchange the DNA bonds many times. The quartz crystal data require some comments. Formally, the use of Sauerbrey equation is justified for thin rigid films. The gels are not very rigid; however, they are very thin. The film should not be too thick, the mass loading should be lower than 2% of the mass of the quartz plate, i.e., typically lower than 20 mg cm^{-2}. In our case the highest mass of the gel deposited was 16 mg cm^{-2}. To make sure that the EQCM data are well interpreted, we compared them with the UV–vis data obtained for the hydrolyzing solution: 0.02 M HEPES buffer of pH 5.5. The amounts of DNA fragments removed from the gel, see Fig. 4, were determined. The agreement was very

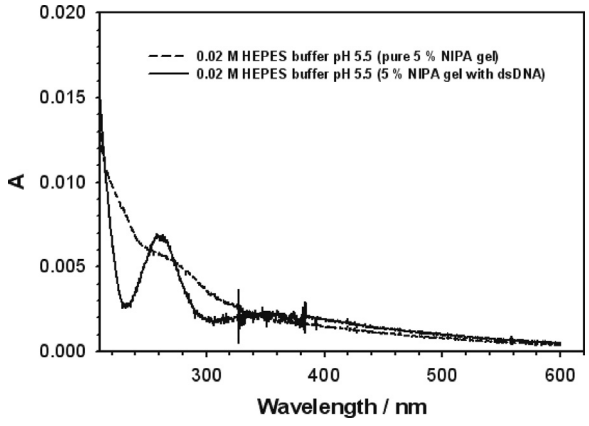

Fig. 4. UV–vis spectra of hydrolyzing solutions after immersing pure gel (NIPA with 5% of –COOH groups) and gel modified by dsDNA in 0.02M HEPES buffer, pH 5.5.

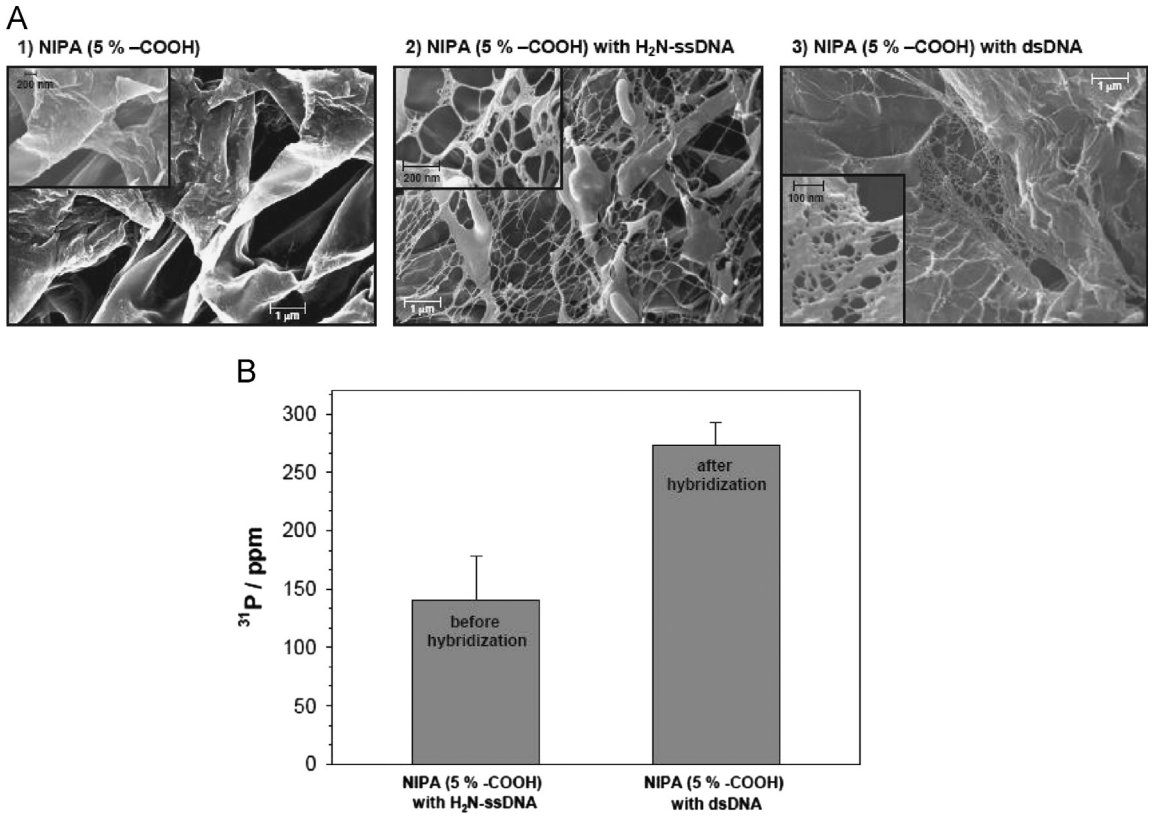

Fig. 5. (A) SEM images of lyophilized pure gel (1) and gel before (2) and after hybridization process (3); (B) contents of ^{31}P in NIPA (5% –COOH) containing DNA before (NIPA 5% –COOH with H_2N-ssDNA) and after hybridization process (NIPA 5% –COOH with dsDNA). The data are pure-gel corrected.

satisfying: 3.09 ± 0.21 (EQCM) vs. $3.04 \pm 0.50 \times 10^{13}$ (UV–vis) DNA molecules.

The changes in the hydrogel morphology before and after hybridization process were analyzed by application of the field emission scanning electron microscopy (FESEM; Merlin; Carl Zeiss Germany). The images were taken at a low primary electron beam energy (5 keV). To preserve the natural structure of the hydrogel the samples were lyophilized. Typical SEM images of the pure hydrogel and after attachment of ssDNA and the hybridization process are shown in Fig. 5A. The introduction of DNA to the polymer matrix led to the filling of the channels in the gel. The hybridization process leads to more complete filling. To control the extent of the hybridization process the content of ^{31}P was determined in gel samples containing ssDNA and dsDNA. The data are presented in Fig. 5B.

The ratio of ^{31}P contents of dsDNA- and ssDNA samples was 1.95 ± 0.4, which means that the hybridization process was nearly 100% efficient (for ideally 100% hybridization the ratio should be 2, since the number of ^{31}P atoms is doubled). In addition: the value of the ^{31}P contents in the swelling gel, determined from the EQCM data, is 2.6 ± 0.4 mg (ssDNA) per 1 kg of the gel (2.6 ppm), while the value determined from LA ICP MS data was 2.2 ± 0.6 ppm. These results also confirm the correctness of conclusions drawn from the EQCM data.

4. Conclusions

It appeared that the NIPA gel containing the carboxyl groups in the range 2.5–5% is a very useful, specific platform for the DNA immobilization. The modification of particular material surface with a thin layer of this polymer allowed us to introduce a one order of magnitude bigger number of DNA strands compared to the traditional, popular intermediary layers such as thiol self-assembly monolayers and phenyl layers. Despite the relatively high density of DNA in the three-dimensional polymer matrix all the DNA strands were capable of taking part in the hybridization process, because each strand got enough free space compared to the traditional matrixes. This is well seen in the SEM images. The QCM, chronoamperometry, LA ICP MS and UV–vis measurements proved that the efficiency of the hybridization process of DNA attached to the polymer chains was very high. The proposed procedure of DNA immobilization goes with the possibility of controlling the thickness of the polymer matrix. This in not easily achieved in the most popular electropolymerization method. In our method the consecutive slices are obtained from one gel rod and, therefore, are of identical composition. Also it is straightforward to handle several gel slices and treat them with different DNA strands.

It appeared that after the experiments the dissociation of immobilized DNA strands was possible in weakly acidic media. This allowed the multiple reuse of the platform. The new findings are important for the biological studies and opens new possibilities in the construction of the DNA sensing platforms of extremely high selectivity. The more DNA strands the higher should be the sensitivity of the sensor. The detection limit has been improved substantially compared to the electrode with a planar sensing layer.

Acknowledgment

This work was supported by the Polish Ministry of Science and Higher Education Grant no. IP2011 025971.

References

Adenier, A., Chehimi, M.M., Gallardo, I., Pinson, J., Vilŕ, N., 2004. Langmuir 20, 8243–8253.

Adhikari, B., Banerjee, A., 2010. Chem. Eur. J. 16, 13698–13705.
Adhikari, B., Banerjee, A., 2011. Soft Matter 7, 9259–9266.
Baeissa, A., Moghimi, N., Liu, J., 2012. RSC Adv. 2, 2981–2987.
Bruckenstein, S., Shay, M., 1985. Electrochim. Acta 30, 1295–1300.
Brug, G.J., Van Den Eeden, A.L.G., Sluyters-Rehbach, M., Sluyters, J.H., 1984. J. Electroanal. Chem. 176, 275–295.
Bard, A.J., Inzelt, G., Scholz, F., 2008. Electrochemical Dictionary. Springer-Verlag, Berlin.
Finklea, H.O., Avery, S., Lynch, M., Furtsch, T., 1987. Langmuir 3, 409–413.
Gallardo, I., Pinson, J., Vilá, N., 2006. J. Phys. Chem. B 110, 19521–19529.
He, X., Wei, B., Mi, Y., 2010. Chem. Commun. 46, 6308–6310.
Hepel, M., 1999. In: Wieckowski, A. (Ed.), Interfacial Electrochemistry. Marcel Dekker, New York, pp. 599–631.
Huang, J., Wu, Y.R., Chen, Y., Zhu, Z., Yang, X.H., Yang, C.Y.J., Wang, K.M., Tan, W.H., 2011. Angew. Chem. Int. Ed. 50, 401–404.
Karbarz, M., Gniadek, M., Stojek, Z., 2005. Electroanalysis 17, 1396–1400.
Kopeček, J., 2007. Biomaterials 28, 5185–5192.
Kowalczyk, A., Nowicka, A.M., Jurczakowski, R., Fau, M., Krolikowska, A., Stojek, Z., 2011. Biosens. Bioelectron. 26, 2506–2512.
Kowalczyk, A., Fau, M., Nowicka, A.M., Stojek, Z., 2012. Electroanalysis 24, 2053–2060.
Lasia, A., 2009. In: Schlesinger, M. (Ed.), Modern Aspects of Electrochemistry. Modeling and Numerical Simulations. Springer, New York, pp. 67–138.
Lide, D.R., Frederikse, H.P.R., 1997. CRC Handbook of Chemistry and Physics. CRC Press, New York.
Liu, J., Gooding, J.J., Paddon-Row, M.N., 2005. Chem. Commun. 5, 631–633.
Lomas, H., Canton, I., MacNeil, S., Du, J., Armes, S.P., Ryan, A.J., Lewis, A.L., Battaglia, G., 2007. Adv. Mater. 19, 4238–4243.
Ogi, H., Fukunishi, Y., Omori, T., Hatanaka, K., Hirao, M., Nishiyama, M., 2008. Anal. Chem. 80, 5494–5500.
Park, H.-Y., Schadt, M.J., Wang, L., Lim, I.I.S., Njoki, P.N., Kim, S.H., Jang, M.-Y., Luo, J., Zhong, C.-J., 2007. Langmuir 23, 9050–9056.
Patolsky, F., Lichtenstein, A., Willner, I., 2000. Angew. Chem. Int. Ed. 39, 940–943.
Pividori, M., Alegret, S., 2005. In: Wittmann, Ch. (Ed.), Immobilization of DNA on Chips I.. Springer-Verlag, Berlin/Heidelberg, pp. 1–36.
Sauerbrey, G., 1959. Z. Phys. 155, 206–222.
Shamsi, M.H., Kraatz, H.-B., 2011. Analyst 136, 3107–3112.
Steichen, M., Decrem, Y., Godfroid, E., Buess-Herman, C., 2007. Biosens. Bioelectron. 22, 2237–2243.
Steel, A., Herne, T.M., Tarlov, M.J., 1998. Anal. Chem. 70, 4670–4677.
Tan, H., Xiao, Ch., Sun, J., Xiong, D., Hu, X., 2012. Chem. Commun. 48, 10289–10291.
Taton, T.A., Mirkin, C.A., Letsinger, R.L., 2000. Science 289, 1757–1760.
Wang, H., Wang, Z., Yi, X., Long, J., Liu, J., Yang, Z., 2011. Chem. Commun. 47, 955–957.
Wang, J., Fernandes, J.R., Kubota, L.T., 1998. Anal. Chem. 70, 3699–3702.
Wang, J., Jiang, M., Mukherjee, B., 2000. Bioelectrochem 52, 111–114.
Yang, T.-H., 2008. Recent Pat. Mater. Sci. 1, 29–40.
Zelikin, A.N., Becker, A.L., Johnston, A.P.R., Wark, K.L., Turatti, F., Caruso, F., 2007. ACS Nano 1, 63–69.
Zhang, W., Yang, T., Jiang, Ch., Jiao, K., 2008. Appl. Surf. Sci. 254, 4750–4756.
Zhou, H., Zhang, Y.-Y., Liu, J., Xu, J.-J., Chen, H.-Y., 2013. Chem. Commun. 49, 2246–2248.